

Wind Turbine Sensor Fault Tolerant Control via a Multiple-Model Approach

Montadher Sami and Ron J Patton

Department of Engineering, University of Hull, Hull HU6 7RX, UK

(e-mail: r.j.patton@hull.ac.uk; M.s.Shaker@2008.hull.ac.uk)

Abstract— This paper presents a new strategy for wind turbine fault tolerant control (FTC) to optimise the wind energy captured by a wind turbine operating at low wind speeds. The FTC strategy uses Takagi-Sugeno (T-S) fuzzy observers with state feedback control to maintain nominal wind turbine control without changes in both the fault and fault-free cases. The proposed strategy obviates the need for sensor fault residual evaluation and observer switching by using a fuzzy proportional multiple integral observer (PMIO) to mask i.e. ‘*implicitly compensate*’ the sensor fault(s) from the controller input and provide good estimation over a wide range of sensor fault scenarios. The proposed FTC method is applied to a 5 MW offshore wind turbine (OWT) benchmark model.

I. INTRODUCTION

Recently, FTC methods have stimulated research in a wide range of industrial control communities and academia, particularly for the systems that demand a high degree of reliability and availability (sustainability) and at the same time are characterised by expensive and/or safety critical maintenance work. The recently developed OWTs are foremost example for these systems having highly non-linear aerodynamics and with a stochastic and uncontrollable driving force as input in the form of wind speed. Moreover, the OWT site accessibility and system availability is not always ensured during or soon after malfunctions, primarily due to changing weather conditions. Indeed, maintenance work for OWTs is more expensive than the maintenance of onshore wind turbines by a factor of 5-10 times [1]. Hence, to be competitive with other energy sources, the main challenges for the deployment of wind turbine systems are to maximise the amount of good quality electrical power extracted from wind energy over a significantly wide range of weather conditions and minimise both manufacturing and maintenance costs.

In the literature, FTC and fault detection and diagnosis (FDD) systems have been recognised as the proper solution of ensuring the above mentioned requirements [2-6].

Specifically, in [5] the authors proposed linear parameter-varying (LPV) FTC systems for pitch actuator faults occurring in the full load operation with more emphasis on controller design rather than on fault estimation. In [6] fuzzy T-S observer based sensor FTC design is proposed to be capable of achieve maximization of wind power extraction. Their proposed FTC method is based on evaluation of *two* residual signals generated using the *generalised observer* idea of [7] to switch the estimation from faulty to healthy observers with the assumption that no simultaneous sensors faults are occur. It is

Montadher Shaker acknowledges funding support for his PhD scholarship from the ministry of higher education and scientific research of Iraq.

clear that switching between two different observers produces unavoidable spikes that specifically affect the drive train torsion of low inertia wind turbines. Also the performance of the proposed FTC strategy is highly affected by the robustness and the computation time of the residual evaluation unit. Moreover, there is a significant probability of simultaneous occurrence of generator and rotor speed sensor faults [2].

This paper describes a new T-S fuzzy observer-based sensor FTC scheme designed to optimise the wind energy captured in the low wind speed range of operation. To cover a wider than usual range of sensor fault scenarios, the FTC strategy uses a fuzzy extension to the well-known PMIO [8] to provide simultaneous estimation of states and sensor faults. The nominal fuzzy controller remains unchanged during faulty and fault-free cases.

The main contributions of the paper are: (1) the use of the PMIO to mask or *implicitly compensate* the effect of drive train sensor faults, hence obviating the need for residual evaluation and observer switching. The PMIO simultaneously estimates the states and the sensor fault signals. Moreover, information about the fault severity can also be provided through the fault estimation signals; (2) the new fuzzy PMIO scheme is shown to cover a wide range of sensor fault scenarios [8].

The paper is organised as follows, Section 2 presents the flexible two mass OWT drive train model Section 3 describes the proposed FTC strategy. In Section 4 simulation results are presented showing the application of the FTC scheme to a 5MW wind turbine benchmark model. Section 5 gives a concluding statement.

II. WIND TURBINE MODELLING

Normally, wind turbine models are obtained by combining the constituent subsystem models that make up the overall wind turbine dynamics. In this section a flexible low speed shaft, two mass wind turbine models are presented. The aerodynamic torque (T_a) representing the source of nonlinearity of the wind turbine. T_a , depending on the rotor speed ω_r , the blade pitch angle β and the wind speed v is given by:

$$T_a = 0.5\rho\pi R^2 C_p(\lambda, \beta) \frac{v^3}{\omega_r} \quad (1)$$

where ρ is the air density, R is the radius of the rotor, and C_p is the power coefficient that depends on the blade pitch angle (β) and the tip-speed-ratio (λ) (TSR) defined as:

$$\lambda = \omega_r R / v \quad (2)$$

The drive train is responsible for gearing up the rotor speed to a higher generator rotational speed. The drive train model includes low and high speed shafts linked together by a

gearbox modelled as a gear ratio. The state space model of the wind turbine drive train has the form:

$$\begin{bmatrix} \dot{\omega}_r \\ \dot{\omega}_g \\ \dot{\theta}_\Delta \end{bmatrix} = \begin{bmatrix} a_{11} & a_{12} & a_{13} \\ a_{21} & a_{22} & a_{23} \\ a_{31} & a_{32} & a_{33} \end{bmatrix} \begin{bmatrix} \omega_r \\ \omega_g \\ \theta_\Delta \end{bmatrix} + \begin{bmatrix} b_{11} & 0 \\ 0 & b_{22} \\ 0 & 0 \end{bmatrix} \begin{bmatrix} T_a \\ T_g \end{bmatrix} \quad (3)$$

where:

$$\begin{aligned} a_{11} &= -\frac{(B_{dt} + B_r)}{J_r} & a_{12} &= \frac{B_{dt}}{n_g J_r} & a_{13} &= -\frac{K_{dt}}{J_r} \\ a_{21} &= \frac{B_{dt}}{n_g J_g} & a_{22} &= -\frac{(B_{dt} + n_g B_g)}{n_g^2 J_g} & a_{23} &= \frac{K_{dt}}{n_g J_g} \\ a_{31} &= 1 & a_{32} &= -\frac{1}{n_g} & a_{33} &= 0 \\ b_{11} &= \frac{1}{J_r} & b_{22} &= -\frac{1}{J_g} \end{aligned}$$

where J_r is the rotor inertia, B_r is the rotor external damping, J_g is the generator inertia, ω_g and T_g are the generator speed and torque, B_g is the generator external damping, n_g is the gearbox ratio, K_{dt} is the torsion stiffness, B_{dt} is the torsion damping coefficient, and θ_Δ is the torsion angle.

It should be noted that the blade pitch subsystem model is not considered here as the pitch angle is held at the optimal pitch angle $\beta = 0$ value during low wind speed range to achieve maximum power extraction. The converter and generator subsystem is not considered here as the proposed controller presented here is designed as an outer controller to provide the inner generator controller with the required reference torque command. This approach to controller design separation is acceptable since the converter-generator subsystem is faster than the aerodynamic subsystem.

III. THE PROPOSED STRATEGY

The nonlinear behaviour of the aerodynamic subsystem and its dependence on wind speed, it is decided to use the T-S fuzzy model based control strategy to design active sensor FTC.

This Section focuses on the description of the proposed active sensor FTC strategy for wind turbine power maximisation. Fig.1 schematically illustrates the proposed strategy.

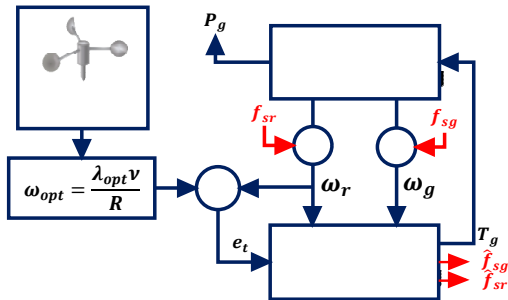


Figure 1: wind turbine sensor FTC scheme

The aim is to tolerate the effects of the drive train sensor fault. An estimator is used to estimate the fault signal and implicitly tolerate its effect on the state estimate signals delivered to the controller input. This strategy can be considered as a *fault-hiding* approach to FTC where the main objective of fault hiding is to maintain the same controller in both faulty and fault-free system cases.

The T-S fuzzy extension to the model given in (3) is:

$$\begin{cases} \dot{x} = A(p)x(t) + Bu + E(p)v \\ y = Cx(t) + D_f f_s \end{cases} \quad (4)$$

The system matrices $A(p) \in \mathcal{R}^{n \times n} (= \sum_{i=1}^r h_i(p)A_i)$, $B \in \mathcal{R}^{n \times m}$, $E(p) \in \mathcal{R}^{n \times m_v} (= \sum_{i=1}^r h_i(p)E_i)$, $D_f \in \mathcal{R}^{l \times g}$ and $C \in \mathcal{R}^{l \times n}$ are known, r is the number of fuzzy rules and the term $h_i(p)$ is the weighting function satisfying $\sum_{i=1}^r h_i(p) = 1$, and $1 \geq h_i(p) \geq 0$, for all i .

Remark1: The system given in Eq.(4) can be obtained from Eq.(3) by linearising the rotor aerodynamic torque equation. The central point to note in the T-S model given in Eq.(4) is that the system has common B and C matrices which will be utilized throughout the derivation of the proposed observer based controller. Details of linearization are given in [6, 9].

An augmented system consisting of the system (4) and the integral of the tracking error $e_t = \int (y_r - Sy)$ is defined as:

$$\begin{cases} \dot{\bar{x}} = \bar{A}(p)\bar{x} + \bar{B}u + \bar{E}(p)v + Ry_r \\ \bar{y} = \bar{C}\bar{x} + \bar{D}_f f_s \end{cases} \quad (5)$$

$$\bar{A}(p) = \begin{bmatrix} 0 & -SC \\ 0 & A(p) \end{bmatrix}, \bar{x} = \begin{bmatrix} e_t \\ x \end{bmatrix}, \bar{B} = \begin{bmatrix} 0 \\ B \end{bmatrix}$$

$$\bar{E}(p) = \begin{bmatrix} 0 \\ E(p) \end{bmatrix}, R = \begin{bmatrix} I \\ 0 \end{bmatrix}$$

$$\bar{C} = \begin{bmatrix} I_q & 0 \\ 0 & C \end{bmatrix}, \bar{D}_f = \begin{bmatrix} 0 \\ D_f \end{bmatrix}$$

where $S \in \mathcal{R}^{w \times l}$ is used to define which output variable is considered to track the reference signal.

Hence, the tracking problem is transferred to a fuzzy state feedback control, for which the proposed control signal is as:

$$u = K(p)\hat{\bar{x}} \quad (6)$$

where $K(p) \in \mathcal{R}^{m \times (n+w)} (= \sum_{i=1}^r h_i(p)K_i)$ is the controller gain and $\hat{\bar{x}} \in \mathcal{R}^{(n+w)}$ is the estimated augmented state vector.

If it is assumed that the q^{th} derivative of the sensor fault signal is bounded, then an augmented state system consisting from the original local linear systems state and the q^{th} derivative of the f_s , can be constructed.

Now let:

$$\varphi_i = f_s^{q-i} \quad (i = 1, 2, \dots, q)$$

$$\dot{\varphi}_1 = f_s^q; \dot{\varphi}_2 = \varphi_1; \dot{\varphi}_3 = \varphi_2; \dots; \dot{\varphi}_q = \varphi_{q-1}$$

Then the system (2) with augmented fault derivatives will become:

$$\begin{cases} \dot{x}_a = A_a(p)x_a + B_a u + E_a(p)v + R_a y_r + G f_s^q \\ y_a = C_a x_a \end{cases} \quad (7)$$

where

$$x_a = [\bar{x}^T \quad \varphi_1^T \quad \varphi_2^T \quad \varphi_3^T \quad \dots \quad \varphi_q^T]^T \in \mathcal{R}^{\bar{n}}$$

$$A_a = \begin{bmatrix} \bar{A} & 0 & \dots & 0 & 0 \\ 0 & 0 & \dots & 0 & 0 \\ 0 & I & \dots & 0 & 0 \\ \vdots & \vdots & \ddots & \vdots & \vdots \\ 0 & 0 & \dots & I & 0 \end{bmatrix} \in \mathcal{R}^{\bar{n} \times \bar{n}}$$

$$B_a = [\bar{B}^T \ 0 \ 0 \ \dots \ 0]^T \in \mathcal{R}^{\bar{n} \times m}$$

$$G = [0 \ I_q \ 0 \ \dots \ 0]^T \in \mathcal{R}^{\bar{n} \times q}$$

$$C_a = [\bar{C} \ 0 \ 0 \ \dots \ \bar{D}_f] \in \mathcal{R}^{l \times \bar{n}}$$

$$\bar{n} = (n + w) + qg$$

Hence, the following T-S fuzzy PMI observer is proposed to simultaneously estimate the system states and sensor faults:

$$\begin{cases} \dot{\hat{x}}_a = A_a(p)\hat{x}_a + B_a u + E_a(p)v + R_a y_r + L_a(p)(y_a - \hat{y}_a) \\ \hat{y}_a = C_a x_a \end{cases} \quad (8)$$

The state estimation error dynamics are obtained by subtracting Eq. (8) from Eq. (7) to yield:

$$\dot{e}_x = (A_a(p) - L_a(p)C_a)e_x + Gf_s^q \quad (9)$$

The augmented system combining the augmented state space system (5), the controller (6), and the state estimation error (9) is given by:

$$\dot{\hat{x}}_a(t) = \sum_{i=1}^r h_i(p) \{ \tilde{A}_i \tilde{x}_a + \tilde{N}_i \tilde{d} \} \quad (10)$$

where:

$$\tilde{A}_i = \begin{bmatrix} \bar{A}(p) + \bar{B}K(p) & -\bar{B}[K(p) \ 0_{m \times q}] \\ 0 & A_a(p) - L_a(p)C_a \end{bmatrix}$$

$$\tilde{x}_a = \begin{bmatrix} \tilde{x} \\ e_x \end{bmatrix}, \quad \tilde{N}_i = \begin{bmatrix} \bar{E}(p) & R & 0 \\ 0 & 0 & G \end{bmatrix}, \quad \tilde{d} = \begin{bmatrix} d \\ y_r \\ f_s^q \end{bmatrix}$$

The objective here is to compute the gains $L_a(p)$ and $K(p)$ such that the effect of the input \tilde{d} in Eq.(10) is attenuated below the desired level γ , to ensure robust stabilisation performance.

Theorem1: For $t > 0$ and $h_i(p)h_j(p) \neq 0$, The closed-loop fuzzy system in (6) is asymptotically stable and the H_∞ performance is guaranteed with an attenuation level γ , provided that the signal (\tilde{d}) is bounded, if there exist symmetric positive definite matrices P_1, P_2 , and matrices H_i, Y_i , and scalar γ satisfying the following LMI constraints (11&12):

Minimise γ , such that:

$$P_1 > 0, \quad P_2 > 0 \quad (11)$$

$$\begin{bmatrix} \Psi_{11} & \Psi_{12} & \bar{E}(p) & R & 0 & 0 & 0 & 0 & 0 & X_1 C_p^T \\ * & -2\mu\bar{X}_1 & 0 & 0 & 0 & \mu I & 0 & 0 & 0 & 0 \\ * & * & -2\mu I & 0 & 0 & 0 & \mu I & 0 & 0 & 0 \\ * & * & * & -2\mu I & 0 & 0 & 0 & \mu I & 0 & 0 \\ * & * & * & * & -2\mu I & 0 & 0 & 0 & \mu I & 0 \\ * & * & * & * & * & \Psi_{55} & 0 & 0 & P_2 G & 0 \\ * & * & * & * & * & * & -\gamma I & 0 & 0 & 0 \\ * & * & * & * & * & * & * & -\gamma I & 0 & 0 \\ * & * & * & * & * & * & * & * & -\gamma I & 0 \\ C_p X_1 & * & * & * & * & * & * & * & * & -\gamma I \end{bmatrix} < 0 \quad (12)$$

where:

$$K_i = Y_i X_1^{-1}, \quad L_a = P_2^{-1} H_{ai}, \quad X_1 = P_1^{-1}, \quad \bar{X}_1 = \begin{bmatrix} X_1 & 0 \\ 0 & I_{q \times q} \end{bmatrix}$$

$$\Psi_{11} = \bar{A}_i X_1 + (\bar{A}_i X_1)^T + \bar{B} Y_i + (\bar{B} Y_i)^T; \quad \Psi_{12} = [-\bar{B} Y_i \quad 0];$$

$$\Psi_{55} = P_2 A_{ai} + (P_2 A_{ai})^T - H_{ai} C_a - (H_{ai} C_a)^T.$$

Proof: From Theorem 1, to achieve the performance and required closed-loop stability of (10) the following inequality must hold [10]:

$$\dot{v}(\tilde{x}_a) + \frac{1}{\gamma} \tilde{x}_a^T C_p^T C_p \tilde{x}_a - \gamma \tilde{d}^T \tilde{d} < 0 \quad (13)$$

where $\dot{v}(\tilde{x}_a)$ is the time derivative of the candidate Lyapunov function ($v(\tilde{x}_a) = \tilde{x}_a^T \bar{P} \tilde{x}_a$, where $\bar{P} > 0$) for the augmented system (10). Using Eq.(10), inequality (13) becomes:

$$\dot{v}(\tilde{x}_a) = \sum_{i=1}^r h_i \{ \tilde{x}_a^T (\bar{A}_i^T \bar{P} + \bar{P} \bar{A}_i) \tilde{x}_a + \tilde{x}_a^T \bar{P} \tilde{N}_i \tilde{d} + \tilde{d}^T \tilde{N}_i^T \bar{P} \tilde{x}_a \} \quad (14)$$

After simple manipulation, inequality (13) implies that the inequality (15) must hold:

$$\begin{bmatrix} \bar{A}_i^T \bar{P} + \bar{P} \bar{A}_i + \frac{1}{\gamma} I & \bar{P} \tilde{N}_i \\ \tilde{N}_i^T \bar{P} & -\gamma I \end{bmatrix} < 0 \quad (15)$$

To be consistent with (10) \bar{P} is structured as follows:

$$\bar{P} = \begin{bmatrix} P_1 & 0 \\ 0 & P_2 \end{bmatrix} > 0 \quad (16)$$

Then after simple manipulation and using the variable change ($H_{ai} = P_2 L_a(p)$) the inequality (15) can be reformulated as:

$$\Pi_{ij} = \begin{bmatrix} \Omega_{11} & -P_1 [\bar{B} K_j \ 0] & P_1 \bar{E}(p) & P_1 R & 0 \\ * & \Omega_{22} & 0 & 0 & P_2 G \\ * & * & -\gamma I & 0 & 0 \\ * & * & * & -\gamma I & 0 \\ 0 & \vdots & (P_2 G)^T & 0 & -\gamma I \end{bmatrix} < 0 \quad (17)$$

where:

$$\Omega_{11} = \bar{A}_i X_1 + (\bar{A}_i X_1)^T + \bar{B} Y_i + (\bar{B} Y_i)^T + \frac{1}{\gamma} C_p^T C_p$$

$$\Omega_{22} = P_2 A_{ai} + (P_2 A_{ai})^T - \bar{H}_i C_a - (\bar{H}_i C_a)^T$$

A single step design formulation of the matrix inequality in (17) is proposed to avoid the complexity of separate design steps characterised by repeated iteration to determine the gains required. Hence, Π_{ij} as shown in (17) becomes:

$$\Pi_{ij} = \begin{bmatrix} \Pi_{11} & \Pi_{12} \\ * & \Pi_{22} \end{bmatrix} \quad (18)$$

where

$$\Pi_{11} = \Omega_{11}; \quad \Pi_{12} = [-P_1 [\bar{B} K_j \ 0] \quad P_1 \bar{E}(p) \quad P_1 R \quad 0]$$

$$\Pi_{22} = \text{lower right block}$$

to do variable change, the following Lemma is required:

Lemma 1. (Congruence) Consider two matrices P and Q , if P is positive definite and if Q is a full column rank matrix, then the matrix $Q * P * Q^T$ is positive definite.

$$\text{Let } Q = \begin{bmatrix} P_1^{-1} & 0 \\ 0 & X \end{bmatrix}, \text{ and } X = \begin{bmatrix} \bar{X}_1 & 0 & 0 & 0 \\ 0 & I & 0 & 0 \\ 0 & 0 & I & 0 \\ 0 & 0 & 0 & I \end{bmatrix}$$

Then $Q * \Pi_{ij} * Q^T < 0$ is also true and can be written as:

$$\begin{bmatrix} P_1^{-1} \Pi_{11} P_1^{-1} & P_1^{-1} \Pi_{12} X \\ * & X \Pi_{22} X \end{bmatrix} < 0 \quad (19)$$

Inequality (19) implies that $\Pi_{22} < 0$ so that the following inequality holds true [11, 12]:

$$(X + \mu \Pi_{22}^{-1})^T \Pi_{22} (X + \mu \Pi_{22}^{-1}) \leq 0 \Leftrightarrow X \Pi_{22} X \leq -2\mu X - \mu^2 \Pi_{22}^{-1} \quad (20)$$

where μ is a scalar.

By substituting (20) into (19) and using the Schur complement Theorem, then (19) holds if the following inequality holds:

$$\begin{bmatrix} P_1^{-1} \Pi_{11} P_1^{-1} & P_1^{-1} \Pi_{12} X & 0 \\ X \Pi_{12} P_1^{-1} & -2\mu X & \mu I \\ 0 & \mu I & \Pi_{22} \end{bmatrix} < 0 \quad (21)$$

After substitution for $\Pi_{11}, \Pi_{12}, \Pi_{12}, \Pi_{22}$ from (18) and by simple manipulation, the LMI in (12) is obtained. This completes the proof.

IV. SIMULATION RESULTS

The simulation of the proposed T-S fuzzy observer based sensor FTC design is based on the wind turbine benchmark system described in [2]. The drive train subsystem is modelled by a two-mass system assuming a flexible low speed shaft. The model is implemented with band-limited measurements noise. The generator sensor faults are represented by two scale factor errors. The scale factors of 1.1 & 0.9 are multiplied by the simulated real generator rotational speeds. The expected fault effects would be a deviation of the wind turbine from the optimal operation.

Remark2: Without loss of generality, the output matrix parametric fault presented in wind turbine benchmark model [2] can be represented as an additive fault in which the fault signal depends on the measured state, as illustrated below:

$$y_f = C_f x = \begin{bmatrix} 1 & 0 \\ 0 & 0.9 \end{bmatrix} \begin{bmatrix} x_1 \\ x_2 \end{bmatrix} = Cx + \begin{bmatrix} 0 \\ 1 \end{bmatrix} (-0.1 * x_2) \quad (22)$$

Hence, parameter changes in the output matrix C can be considered as a special case of additive faults in which the fault signal (f_s) is a scaled version of the measured state.

Remark3: The sensor fault considered has a direct effect on the wind energy conversion efficiency since the controller starts to drive the wind turbine away from its optimal operation. Noticeably, in spite that this fault involves no damage risk, a study presented in [13] shows that a specific wind turbine operation in a 100 MW rated wind farm and operating with a realistic 35% capacity factor can generate about 307 GWh of energy in a given year. If the cost of the energy is \$0.04 per kWh, each GWh is worth about \$40,000,

meaning that a 1% loss of energy on this wind farm corresponds to a loss of \$123,000 per year.

Fig. 2 shows the expected effects of the sensor bias fault on the power conversion efficiency. In fact, this sensor fault scenario simulates the effect of C_p uncertainty encountered in the standard control law since in both cases the control signal drives the turbine away from the optimal trajectory.

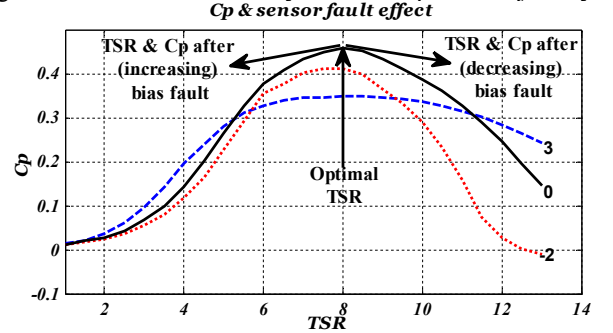


Figure 2: Effects of bias sensor fault on C_p [$\beta = -2, 0, 3$]

Fig. 3 shows how the wind turbine operation is affected by the two fault scenarios and helps to illustrate the success of the proposed strategy to tolerate the effects of the sensor faults, maintaining optimal wind turbine operation.

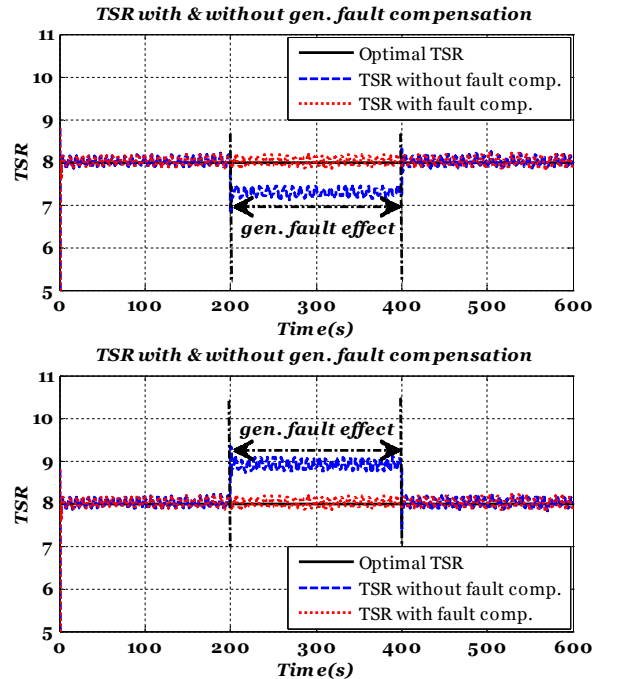


Figure 3: Effect of 1.1 (upper) and 0.9 (lower) sensor bias faults with(out) fault compensation

It is clear that the 1.1 bias sensor fault causes a deceleration of ω_r & ω_g . Based on the faulty measurement the controller forces the turbine to reduce the rotational speed by increasing the reference generator torque which in turn increases the drive train load. This fault scenario is shown in Fig. 5 without sensor fault compensation.

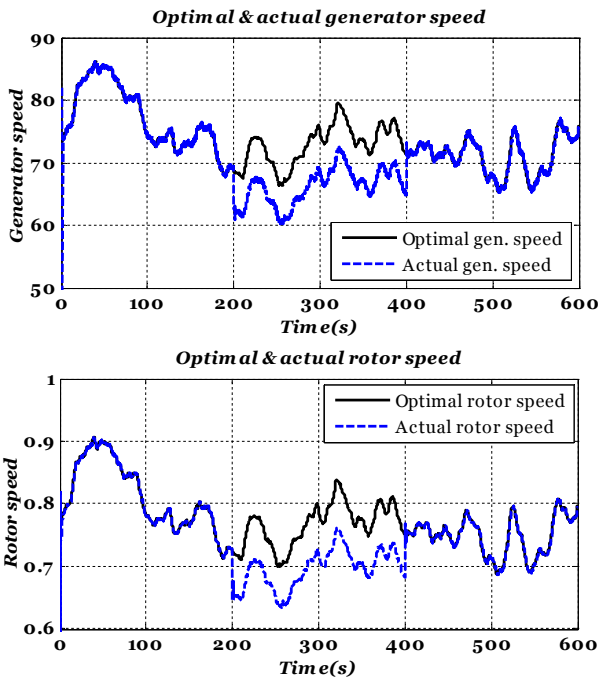


Figure 4: 1.1 sensor bias fault decelerate ω_r & ω_g

On the other hand Fig. 6, shows the time variations of ω_r & ω_g in response to the proposed sensor FTC strategy.

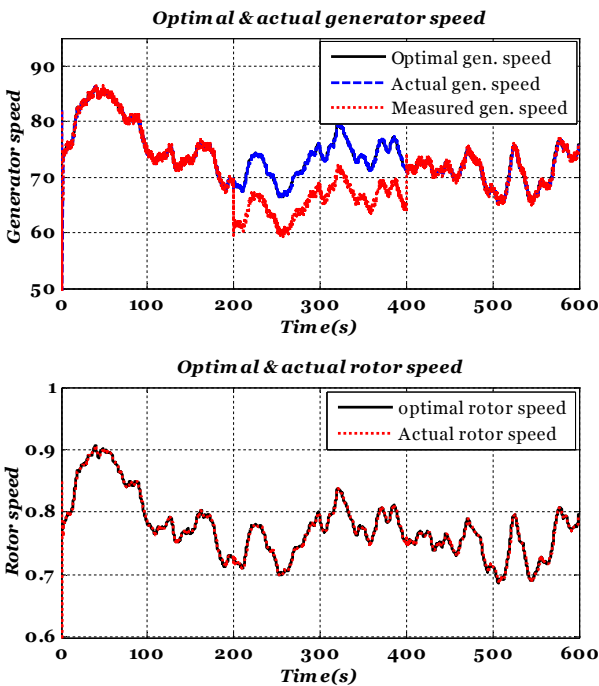


Figure 5: Actual and optimal ω_r & ω_g using the proposed sensor FTC strategy

Conversely, the 0.9 bias sensor fault causes acceleration of ω_r & ω_g since, based on faulty measurement; the controller releases the aerodynamic subsystem to rotate according to the available wind speed. Fig 7 shows the effect of the 0.9 sensor fault without compensation.

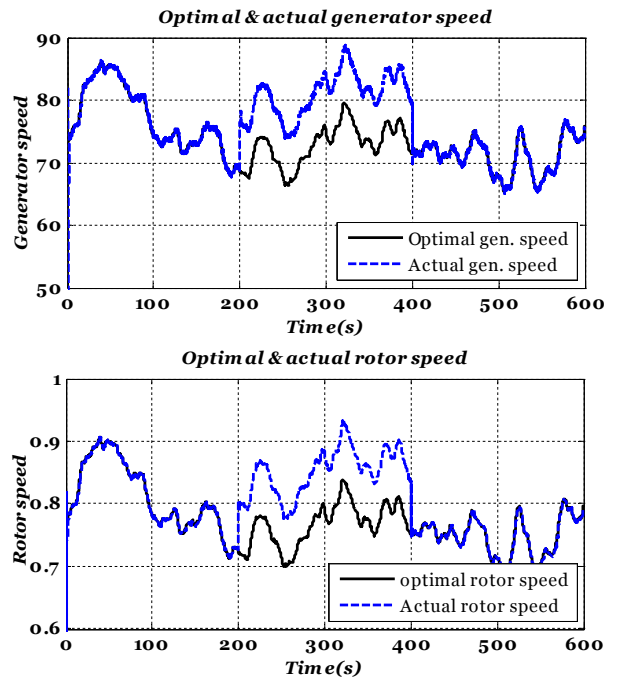


Figure 6: 0.9 sensor bias fault accelerate ω_r & ω_g

The fault estimation signals for both sensor fault scenarios are shown in Fig.7.

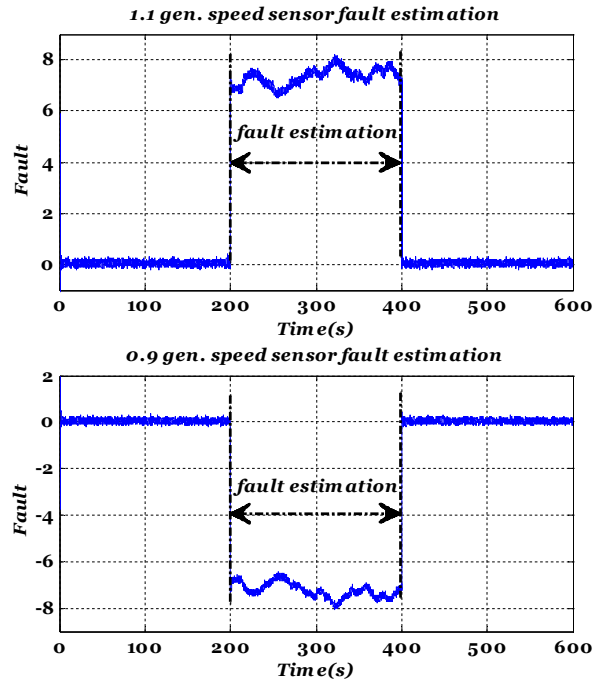


Figure 7: Estimation of 1.1 (upper) and 0.9 (lower) sensor bias faults

The use of the PMIO can also help to produce information about the severity of each fault. This is achieved through taking the ratio between the measured generator speed and the estimated signal. Hence, if there are no faults the ratio should be 1 otherwise any deviation from unity indicates the occurrence of the fault and the magnitude of the deviation represents the fault severity. Fig. 8 shows the fault evaluation signal for both fault scenarios.

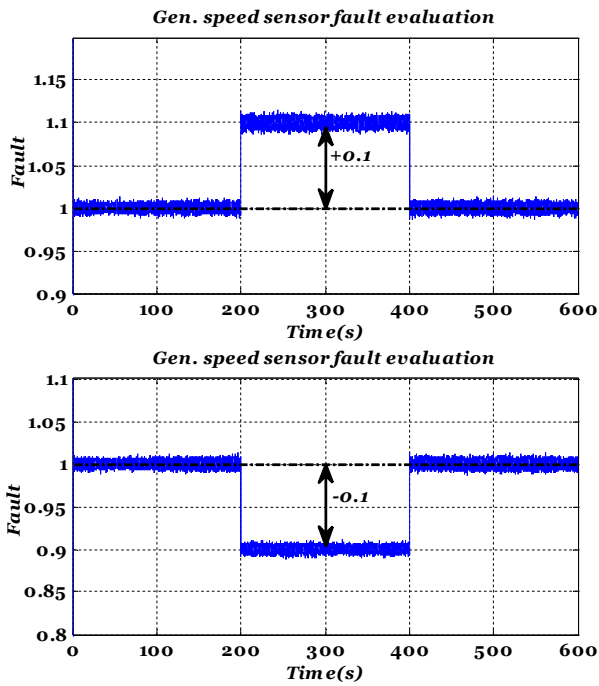


Figure 8: Deviation of 1.1 (upper) and 0.9 (lower) sensor measurement from unity

Remark4: Note that maintaining state estimation without changes during the whole range of operation is due to the fact that the PMIO perform *implicit fault estimation and compensation* of sensor fault from the input of PMIO. This fact is clearly interpreted from the error signal $(y_a - C_a \hat{x}_a)$ which can be rewritten as $(\bar{C}\bar{x} + \bar{D}\bar{f}_s - \bar{C}\bar{x} - \bar{D}\bar{f}_s)$, then as long as there are no sensor faults, $\bar{f}_s = 0$. However, once a sensor fault occurs the fault estimation \hat{f}_s compensates the effect of the fault signal f_s and hence the observer always receives a fault-free error signal.

V. CONCLUSION

OWTs are complex and nonlinear systems that are driven by a stochastic and uncontrollable wind force and require a high degree of reliability and availability (sustainability). OWTs are also characterised by expensive and/or safety critical maintenance work. The main challenges for the deployment of wind turbine systems are to maximise the amount of good quality electrical power extracted from wind energy over a significantly wide range of weather conditions and minimise both manufacturing and maintenance costs. This paper has shown that active FTC can be of potential benefit as a very suitable solution for ensuring wind turbine reliability and sustainability requirements, particularly for offshore wind farms. This is illustrated through the use of the T-S extension to the well known PMIO fault estimation method in the observer based control strategy. However, OWTs are derived by uncontrollable signal in the form of effective wind speed which is not precisely measured due to the large vertical profile of blade swept area. Therefore, robustness of the FTC against this uncertain measurement is the direction of future work. Moreover, tolerate the effect of simultaneous actuator and sensor faults is the other direction of research in this field.

- [1] G. J. W. van Bussel and M. B. Zaaijer, "Reliability, Availability and Maintenance Aspects of Large-Scale Offshore Wind Farms, a Concepts Study," in *MAREC 2001 Marine Renewable Energies Conference*, Newcastle, 2001, pp. 119-126.
- [2] P. F. Odgaard, J. Stoustrup, and M. Kinnaert, "Fault Tolerant Control of Wind Turbines: a Benchmark Model," presented at the 7th IFAC Symposium on Fault Detection, Supervision and Safety of Technical Processes *Safeprocess 2009*, Barcelona, Spain, 2009.
- [3] Y. Amirat, M. E. H. Benbouzid, E. Al-Ahmar, B. Bensaker, and S. Turri, "A brief status on condition monitoring and fault diagnosis in wind energy conversion systems," *Renewable and Sustainable Energy Reviews*, vol. 13, pp. 2629-2636, 2009.
- [4] Z. Hameed, Y. S. Hong, Y. M. Cho, S. H. Ahn, and C. K. Song, "Condition monitoring and fault detection of wind turbines and related algorithms: A review," *Renewable and Sustainable Energy Reviews*, vol. 13, pp. 1-39, 2009.
- [5] C. Sloth, T. Esbensen, and J. Stoustrup, "Robust and fault-tolerant linear parameter-varying control of wind turbines," *Mechatronics*, vol. 21, pp. 645-659, 2011.
- [6] E. Kamal, A. Aitouche, R. Ghorbani, and M. Bayart, "Robust Fuzzy Fault-Tolerant Control of Wind Energy Conversion Systems Subject to Sensor Faults," *IEEE Transactions on Sustainable Energy*, vol. 3, pp. 231-241, 2012.
- [7] R. J. Patton, P. M. Frank, and R. N. Clark, *Fault Diagnosis in Dynamic Systems: Theory and Application*: Hemel Hempstead, UK, Prentice Hall International, 1989.
- [8] Z. Gao, S. X. Ding, and Y. Ma, "Robust fault estimation approach and its application in vehicle lateral dynamic systems," *Optimal Control Applications and Methods*, vol. 28, pp. 143-156, 2007.
- [9] T. Esbensen, B. T. Jensen, M. O. Niss, C. Sloth, and J. Stoustrup, "Joint Power and Speed Control of Wind Turbines," Aalborg University, Aalborg 120, 2008.
- [10] S. X. Ding, *Model-based Fault Diagnosis Techniques Design Schemes, Algorithms, and Tools*: Springer-Verlag Berlin Heidelberg, 2008.
- [11] T. M. Guerra, A. Kruszewski, L. Vermeiren, and H. Tirmant, "Conditions of output stabilization for nonlinear models in the Takagi-Sugeno's form," *Fuzzy Sets and Systems*, vol. 157, pp. 1248-1259, 2006.
- [12] B. Mansouri, N. Manamanni, K. Guelton, and M. Djemai, "Robust pole placement controller design in LMI region for uncertain and disturbed switched systems," *Nonlinear Analysis: Hybrid Systems*, vol. 2, pp. 1136-1143, 2008.
- [13] K. E. Johnson, "Adaptive torque control of variable speed wind turbines," NREL/TP-500-36265, National Renewable Energy Laboratory NREL/TP-500-36265, 2004.